in vitro DNA Binding, Anticancer and Molecular Docking Studies of New Sydnone Compounds

SYED LIDIA HOSSAIN[1], MANOJ MATHEWS[2], B.N. VEERABHADRASWAMY[3],
B. KIRANKUMAR[4], C.V. YELMAGGAD[3] and C. RAJENDRA SINGH[1,*]

[1]Department of Biotechnology, Sir M. Visvesvaraya Institute of Technology, Bangalore-562157, India
[2]Department of Chemistry, St. Joseph's College (Autonomous), Devagiri, Calicut -673008, India
[3]Centre for Nano & Soft Matter Science, Bangalore-562162, India
[4]Department of Biotechnology, SEA College of Science, Commerce and Arts, K.R. Puram, Bangalore-560049, India

*Corresponding author: E-mail: rajendrabiochem@gmail.com

Sydnones have been a novel class of mesoionic compound due to versatility of their applications in various fields. Sydnone derivative have seen as an interesting structure grouped in the heterocyclic community, which is having regions of both positive and negative charges linked with a poly-heteroatomic system. This structural characteristic allows them to cross biological membranes and interact with biomolecules. Four sydnones namely 3-(4-decyloxybiphenyl-4′-yl) sydnone (MC-176), 3-(4-octyloxy-2,3-difluorobiphenyl-4′-yl) sydnone (MC-192), 3-(4-biphenyl-4′-yl) sydnone (MC-450) and 3-(4-butylbiphenyl-4′-yl) sydnone (MC-456) were evaluated for biophysical interactions between DNA and sydnones and antiproliferative activity. The UV-visible spectroscopic study indicates interaction between sydnone and dsDNA with a slight red and hypochromic shift in absorption spectra, which shows the intercalation mode of binding. The binding constant of DNA-Sydnone complexes were in the range from 1.4×10^4 M^{-1} to 7.1×10^4 M^{-1} for different sydnone compounds (MC-176, MC-192, MC-450, MC-456). FTIR spectra indicated that sydnone interaction with DNA occurs through base pairs and the phosphate backbone of the DNA. The cytotoxic and apoptotic effects of a sydnone derivatives on human cervical cancer (HeLa) and breast tumor (BT) 474 cancer cell lines were determined. The compounds possess antiproliferative activity in a concentration-dependent mode. The changes of morphological characteristic of cancer cells were determined by fluorescent staining techniques indicate the apoptotic cell death. The molecular docking studies of sydnone compounds with caspase 3 and EGF-TK showed better interactions (according to docking score) along with commercially available breast cancer drug molecule anastrozole. The docking score of sydnone molecules (MC-456, MC-450, MC-192 and MC-176) with EGF-TK enzyme were -6.44, -6.42, -5.46 and -4.53, respectively. The binding energy of anastrozole with EGF-TK was -6.41. As well Caspase 3 inhibition with sydnone compounds MC-456, MC-450, MC-192 and MC-176 were -6.09, -6.48, -5 and -3.49, respectively. The binding energy of anastrozole with caspase 3 was -6.24. All sydnone compounds were studied for ADME toxicity studies along with Lipinski rule of five to assess their drug likeness properties by *in silico* approach. MC-450 found to have good ADMET (absorption, distribution, metabolism, excretion and toxicology) properties among all the sydnone compounds. Thus, the present work indicates that these sydnone compounds would be a well prospective in developing anticancer medicines.

Keywords: Sydnone, Liquid crystal, Apoptosis, Cell lines, Molecular docking.

INTRODUCTION

Cancer is the one of most eminent diseases in the world causes death around 9.6 million death cases reports were reported in 2018. According to WHO reports occurring and death cases of cancer showing around 70% in middle and low-income countries [1]. Cervical cancer and breast cancer are common among most of the cancers seen in women throughout the globe [2]. Chemotherapeutic drugs are essential to fight against cancer, which has helped the humans to lead quality life. Over the ancient and earlier days, the health issues are under risk because of generally used chemotherapeutic drugs to treat cancer has been less effective due to increase in drug resistant and also many of them have adverse reactions [3]. It is crucial to explore new molecules to treat the cancer and other diseases. Recently many scientists have showed a path in drug discovery by the biological properties of liquid crystal pharmaceutical (LCP). The LCP molecule Tolectin was identified as effective against

antitumor, antibacterial, antiviral properties was explained by Tsai *et al.* [4]. Sydnone derivatives having liquid crystalline properties, that flow like liquids but maintain some of the ordered structured of its molecules [5]. Due to their versatile applications, sydnone molecules have interesting structures inside the heterocyclic community, which is having regions of both positive and negative charges linked with a poly-heteroatomic system, these structural characteristics allow them to cross biological membranes and interact with biomolecules [6].

The changes in normal cell cycle regulation and also changes in apoptosis related genes can lead to cancer and associated to cancer progression [7,8]. Certain drugs proved to be cytotoxic by inducing apoptotic pathway that has the possible effective towards treating cancers [9]. Around 20 million compounds were documented, out of them half are heterocyclic compounds [10]. It is reported that sydnone have a significant cytotoxic against sarcoma 180, *Ehrlich carcinoma* and B10MCII fibrous histiocytoma [11]. It is assumed that anticancer drugs also showed its cytotoxicity by inhibiting the functioning of biological molecules like DNA and related proteins involved in cell cycle. The DNA which replicates rapidly in the cancer cells, the incorporation of DNA binding compounds like alkylating drugs, which disrupts DNA helical structure causing strand breakage and chromosome abnormalities. DNA is an important target for most of the anticancer drugs [12]. Thus, the biophysical interaction of small molecule with dsDNA can be studied by the spectroscopic techniques.

The small molecule can interact to DNA by different modes like intercalation, external binding, major groove binding and minor groove binding. The groove binding and intercalation modes are very common for small molecules to interact with DNA. When an aromatic molecule stacks in the base pairs by electrostatic interactions, intercalation occurs [13]. Many heterocyclic aromatic molecules with cationic tails and extended NH and H-groups can bind to DNA bases in major and minor grooves by hydrogen bonding and electrovalent interactions. DNA-molecule interaction depends on the structural properties of both molecule and DNA [14]. One of the main requirements is DNA should have crescent shape which is compatible to the minor groove curvature [15]. Many molecules show more than a single interaction mode. Recently, UV-Vis and FTIR spectroscopy has developed as an important tool in life sciences for studying molecular interaction [16]. However, UV and FTIR spectroscopy can be used for profound study of DNA-sydnone interaction.

The bioactivity of new sydnone molecules were not much explored for anticancer property [17]. There is a need for developing compounds that induces apoptosis in cancer cells that could be used in cancer therapy. Interestingly sydnone molecules can cross biological membranes and interact with biomolecules, which could be a target site for cancer studies. There are several reasons which affect the drug like property during drug development. It is reported that one of the important causes of failure is related with imperfect pharmacokinetics or ADME toxicity properties [18], which are very important factors for the clinical success of the drug [19]. Sydnone compounds ADME-toxicity properties are predicted computation-

ally. In addition, sydnone compounds were docked with two proteins (Caspase 3 and EGF-TK) by molecular docking study which helps us to understand the binding interaction between sydnone ligands and the receptors. Epidermal Growth Factor Receptor Tyrosine Kinase (EGF-TK) and Caspase 3 are the tumourassociate proteins, which is highly expressed during uncontrolled cell proliferation.

Hence, our aim in this research work is to study the *in vitro* DNA binding studies of sydnones by spectroscopy techniques. The apoptotic potential of the active compounds by fluorescence staining (annexin V-propidium iodide staining method followed by DAPI staining), docking study and ADME toxicology studies are also evaluated.

EXPERIMENTAL

DNA collection and preparation: Type I calf-thymus DNA (highly polymerized) were procured from Sigma Chemicals. The protein content of DNA solution was measured OD at 260 and 280 nm. The A260/A280 ratio was 1.85, which indicate that the DNA was protein free [13]. The homogeneous solution of DNA stocks (1%) was prepared by dissolving 10 mg/mL in buffer (phosphate -pH 7.2) to give 1% (w/v) with intermittent stirring. The DNA stock solution (25 mM) was calculated by using molar extinction coefficient of 6600 cm^{-1} M^{-1} (expressed as molarity of phosphate groups) at 260 nm. The working solutions of DNA were prepared accordingly by diluting the stock using the phosphate buffer.

Sydnone derivatives: Four sydnone compounds were provided by Centre of Nano and soft Matter Science (CENS), Bengaluru, India. The structural details of sydnone compounds are given in Table-1. The stock solutions of sydnone (20 mM) were prepared in 1% DMSO.

UV analysis: The DNA concentration (40 μM) kept constant while changing the sydnone derivatives concentration (20, 40, 60, 80 and 100 μM). The different combination of DNA-sydnone were incubated at room temperature for 30 min and absorption spectra were taken between 200 to 800 nm using a UV-visible light spectrophotometer. The spectral results were recorded by Perkin-Elmer's, Lambda 20 UV-visible spectrophotometer. The sydnone-DNA binding constant were calculated by the following equations [20]:
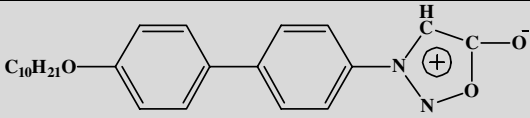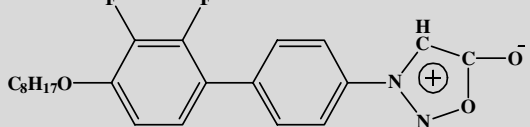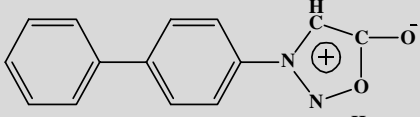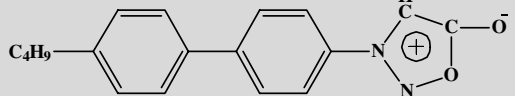
$$DNA + sydnone = DNA - sydnone\ complex,$$

$$K = \frac{DNA - Sydnone\ complex}{[DNA]_{uncomplexed}[sydnone]_{uncomplexed}}$$

The absorbance of only DNA at 260 is A_0, the final absorbance of the DNA-sydnone is A and the absorbance of only sydnone concentrations is A_1. The binding constant (K) was calculated from the double reciprocal plot of $1/(A–A_0)$ *versus* 1/DNA.

FTIR analysis: Perkin-Elmer spectrometer (Spectrum 400) using ATR accessory (ZnSe cell) was used to record the infrared spectra. The spectra were measured in triplicate after 30 min incubation of sydnone (0.8 mM) with DNA (12 mM) solution. Interferograms were collected over a spectrum ranging from 2000 to 600 cm^{-1} with minimal resolution of 2 cm^{-1}. Water subtraction was effectively done as shown by a flat baseline

Compound's code	2D Structure	m.w.	Chemical name
MC-176		396.53	3-(4-Decyloxybiphenyl-4'-yl) sydnone
MC-192		404.46	3-(4-Octyloxy-2,3-difluorobiphenyl-4'-yl) sydnone
MC-450		240.26	3-(4-Biphenyl-4'-yl) sydnone
MC-456		296.27	3-(4-Butylbiphenyl-4'-yl) sydnone

TABLE-1
CHEMICAL STRUCTURE OF SYDNONE DERIVATIVES

around 2200 cm^{-1} using with 50 mM phosphate buffer (pH 7.2) as a reference. ORIGIN software was used to process the spectra.

MTT cell proliferation assay: The cell culture medium components were procured from Hi-media laboratories. Foetal bovine serum (FBS) was acquired from Invitrogen (US). Human cancer cells, BT 474 and the HeLa cell lines were sub-cultured and then used to screen the cytotoxicity after exposure to the compound. Dulbecco's Modified Eagle's medium (DMEM) added with 10% FBS was used to culture the cancer cell lines at 5% CO_2 and 37 ºC. At 85% convergence, the cells were collected and seeded in 96 well plates and permitted to 70% adhere to the surface before treatment. Sydnone stock solutions (20 mM) were made and diluted to the required concentrations for treatment.

The MTT (3-(4,5-dimethylthiazolyl-2)-2,5-diphenyltetrazolium bromide) assay measures the cell division rate and cell viability reduction. Blue colour formazon crystals formed by reducing yellow compound MTT by mitochondrial dehydrogenases, depending on the cell viability. BT 474 breast cancer and the HeLa carcinoma cell (2×10^4 cells/mL) were seeded in 96-well plates and treated with different concentrations (100, 33.3, 11.11, 3.70, 1.23, 0.41, 0.14, 0.05 µM) of sydnones for a period of 24 h (in MTT assay the sydnone concentrations were taken by increasing 3-folds from the initial concentration). After incubating with sydnones, MTT reagent were added and kept in dark for 3-4 h at 37 ºC, resulting in the formation of dark purple formazon crystals. After the solubilization of these crystals with isopropanol, absorbance was taken at 595 nm spectrophotometrically. The experiments were done in triplicate. The percentage of cell viability was calculated as follows:

$$\text{Viability (\%)} = \frac{\text{O.D. of treated cell} - \text{O.D. of blank}}{\text{O.D. of control} - \text{O.D. of blank}} \times 100$$

DAPI (4′,6-diamidino-2-phenylindole) staining: Cell nuclear morphology was assessed by fluorescence microscopy followed by DAPI staining. Human cervical cancer (HeLa) and BT 474 breast cancer cell lines cells were treated with the sydnone compounds (IC_{50} values) for 24 h. The cells were set with 70% ethanol (ice cold) after washing with PBS (pH 7.4). After that DAPI stain was added and kept for 15 min at 37 ºC. The cells were observed under Nikon Eclipse Fluorescence microscope (Nikon Instruments Inc., Japan) after washing with PBS and photographed.

Apoptosis assay (Annexin V and propidium iodide (PI) staining): Necrosis and apoptosis cell death will be distinguished by the Annexin V-FITC and propidium iodide kit (Sigma-Aldrich) by using fluorescent microscopy. After washing with PBS as mentioned in DAPI staining, the annexin V and PI stains were added to the cells according to the instructions of the kit used (BD-Bioscience-Catalogueno. 556547). The stained cells were analyzed and pictures were taken under an Eclipse 50i Nikon fluorescent microscope.

Ligand, protein preparation and active site prediction: Sydnone compound's structures were drawn by ChemDraw software and converted to PDB format by smile converter. The target proteins Caspase 3 (PDB ID - 5I9B) and Epidermal Growth Factor Receptor tyrosine kinase domain (EGF-TK, PDB ID - 1M17) were retrieved from Protein Data Bank (www.rcsb.org) and the water molecules was removed from the protein. A commercially available anti breast cancer drug molecule Anastrozole (PubChem CID: 2187) accessed from PubChem Data base. CASTp server was used to predict the active site of the proteins [21].

Optimization of drug likeliness by Lipinski rule and molecular docking analysis: The compounds structures were drawn by ChemDraw software and evaluated for their drug likeliness by "Lipinski rule of five" [22] (chemine tools open babel software library [23]). Docking studies were carried out between the crystal structure of the proteins (Caspase 3 and EGF-TK) and the four sydnone compounds (ligands) by using AutoDock Tools 1.5.6. The protein and ligand files were converted to "pdbqt" format and grid parameters were set as per the result provided by CASTp. Docking parameters were default selected according to Autodock4 [24]. The docked results

were visualized by Molegro Molecular Viewer and PyMOL (Version 2.0 Schrödinger, LLC) as well the protein-ligand inter-actions were analyzed by Proteins Plus [25] and Protein-Ligand Interaction Profiler (PLIP) [26,27].

ADME Toxicity prediction: All four sydnone compounds were subjected to predict pharmacokinetics properties like absorption, distribution, metabolism, excretion and toxicology (ADMET) with online pkCSM webserver with the canonical smiles of sydnone compounds.

RESULTS AND DISCUSSION

UV-vis studies: For interaction studies between the bio-molecule like DNA and small molecule, commonly used basic analytical instrument is the UV-vis spectroscopy [28,29]. Mole-cules containing functional chromophore group or aromatic substituent might interact with DNA. The interaction between DNA and molecule can be studied by comparing absorption spectra before and after treatment with molecules, which forms the complex [30,31]. The change in absorbance spectra shows the hypochromic or hyperchromic effect and/or shift in the wavelength from red or blue shift will be seen after DNA-sydnone complex formation. The change of spectra suggests

the mode of interactions like groove binding, electrostatic and intercalation [32]. If interaction is strong between them *i.e.* intercalation and the weak interaction indicate electrostatic because of charges or may be groove binding. The red shifts were observed in these interactions with reduce intensity of absorption.

The interaction studies between the sydnone compounds (MC-176, MC-192, MC-450 and MC-456) and ds-DNA was investigated by implementing the absorption titration method. Fig. 1 shows the free calf thymus DNA and absorption spectra, sydnones and sydnone-DNA complexes with different sydnone concentrations (20 μM to 100 μM) with DNA concentration (20 μM). Fig. 1 shows the changes in spectra which indicate the interaction. This interaction is because complex between sydnone-DNA.

Sydnone compounds has an absorption peak at 290-310 nm in spectra. The decreased absorption is considerably seen in MC-176 and MC 450, found to be a hypochromic shift after the complex formation. Also, there was a small change in shift seen towards red end of the spectrum (red shift) *i.e.* bathochromic shift. These changes in shift suggest an inter-calative mode of interaction between compound MC176,
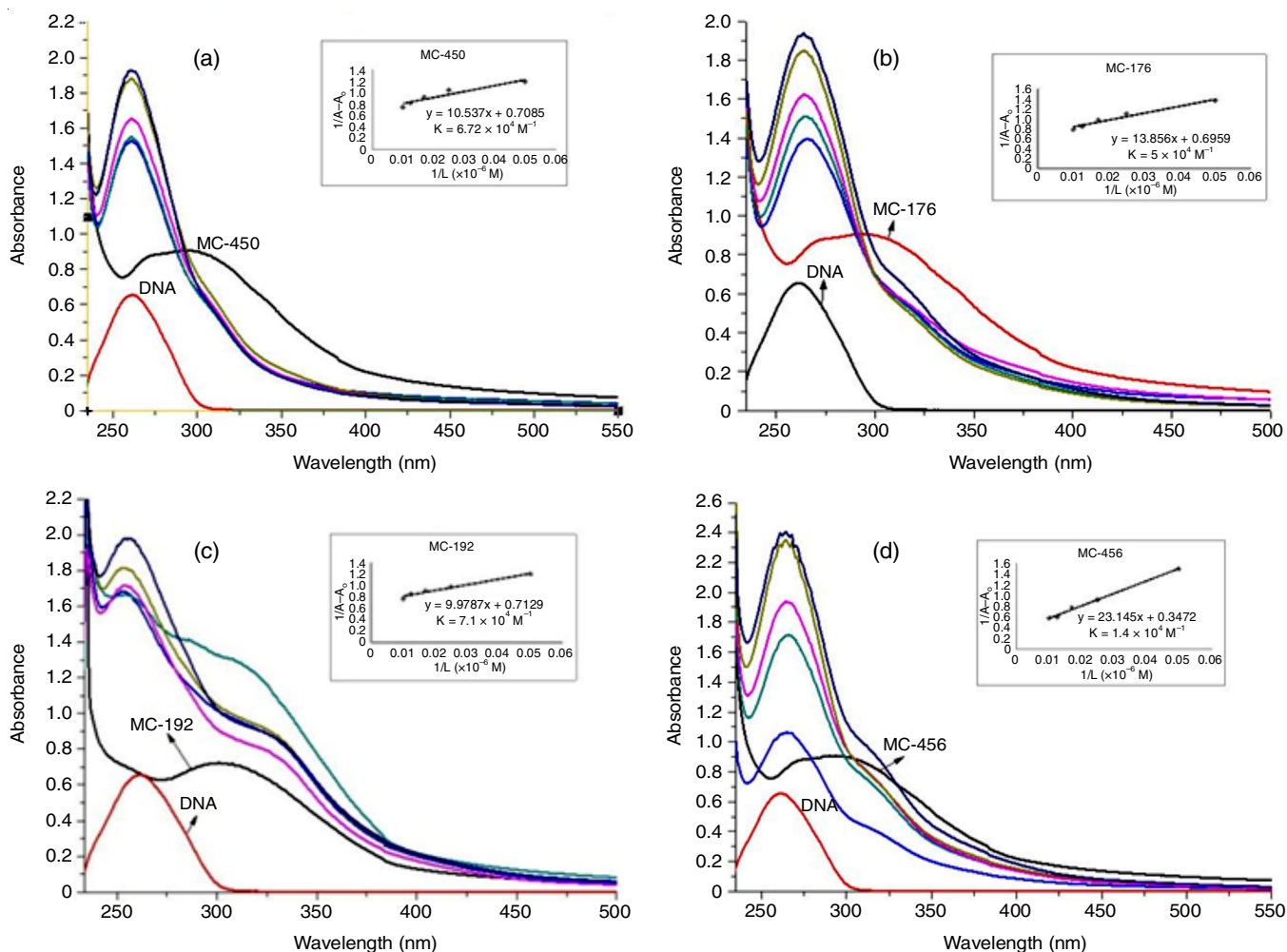

Fig. 1. Spectra of sydnone-DNA binding studies by UV-vis spectroscopy [a, b, c and d represent the UV-vis absorption spectra of free DNA (40 μM) and sydnone-DNA complex (A:MC 176, B:MC 192, C:MC450, D:MC 456 with concentration ranging from 20, 40, 60, 80, 100 μM)]

MC450 and DNA. The MC-192 induces hyperchromic and red shift and MC-456 showed both hypochromic and hyperchromic shifts, these result show intercalation into the double helix of DNA at concentration above 20 µM and also shows the hyperchromic effect, similar effect was also reported by Almeida *et al.* [33]. The absorption spectra of MC 456-DNA complex increases with increasing sydnone concentration, which suggests that the double stranded DNA is altered after interaction with sydnone MC 456 through intercalation mode. In spectral data at 260 nm, the sydnone-DNA complex shows high optical density (OD) for DNA than the corresponding native DNA at the same wavelength. Increased OD indicates that sydnone interact with DNA and induces perturbations in DNA conformation. Some reports shown that heterocyclic quinolone compounds bind to CT-DNA *via* intercalation in similar mode [34]. In general, absorption decreased (hypochromic effect) or increased (hyper chromic effect) and as light shift of peak towards higher wavelength region (bathochromic effect), indicating the interaction (intercalation) between sydnone and DNA.

The intercalation phenomena of the sydnone with DNA could be explained by the electronic transitions. The mode of binding of sydnones (MC-176, MC-192, MC-450 and MC-456) to DNA is by intercalation seen in both hypochromic and bathochromic shifts. The intercalative interaction was seen between sydnone aromatic chromophore and DNA stacked base pairs (AT GC). The intensity of hypochromic effect is depending upon relative strength of intercalative interaction. The degree of interaction is depending upon distance between chromophore and aromatic purine and pyrimidine bases in DNA. By lessen the space between them leads to hypochromic shift. This may also depend upon the presence of π-electrons in sydnone and bases in DNA. Hence, the energy levels of π and π* falls to see red shift [35]. These reasons suggest that sydnone compounds (MC-176, MC-192, MC-450 and MC-456) bind to DNA by intercalation. In DNA and sydnone (MC-192) complex, hyperchromic and red shift were observed, which indicates change in DNA conformation and structure. This hyperchromic effect is because of denaturation of DNA.

Based on the UV-vis spectra of sydnone-DNA complex as shown in Fig. 1, the binding constant (K) was determined and found to be of 5×10^4 M^{-1} for MC-176, 7.1×10^4 M^{-1} for MC-192, 6.72×10^4 M^{-1} for MC-450 and 1.4×10^4 M^{-1} suggested a strong affinity to CT-DNA.

Sydnone-DNA complex FTIR spectra: It was observed that change in intensity and shifting of the peaks in DNA vibrations of sydnone-DNA complex. Particularly, the vibration in DNA were observed at 1711 cm^{-1} (Gua), 1649 cm^{-1} (Thy), 1601 cm^{-1} (Ade), 1486 cm^{-1} (Cyt). For phosphate, the peaks are observed at 1217 cm^{-1} (PO$_2$ asymm. *str.*) and 1096 cm^{-1} (PO$_2$ asymm. *str.*) [35] were observed for all four sydnone compounds (MC-176, MC-192, MC-450, MC-456) as shown in Fig. 2.
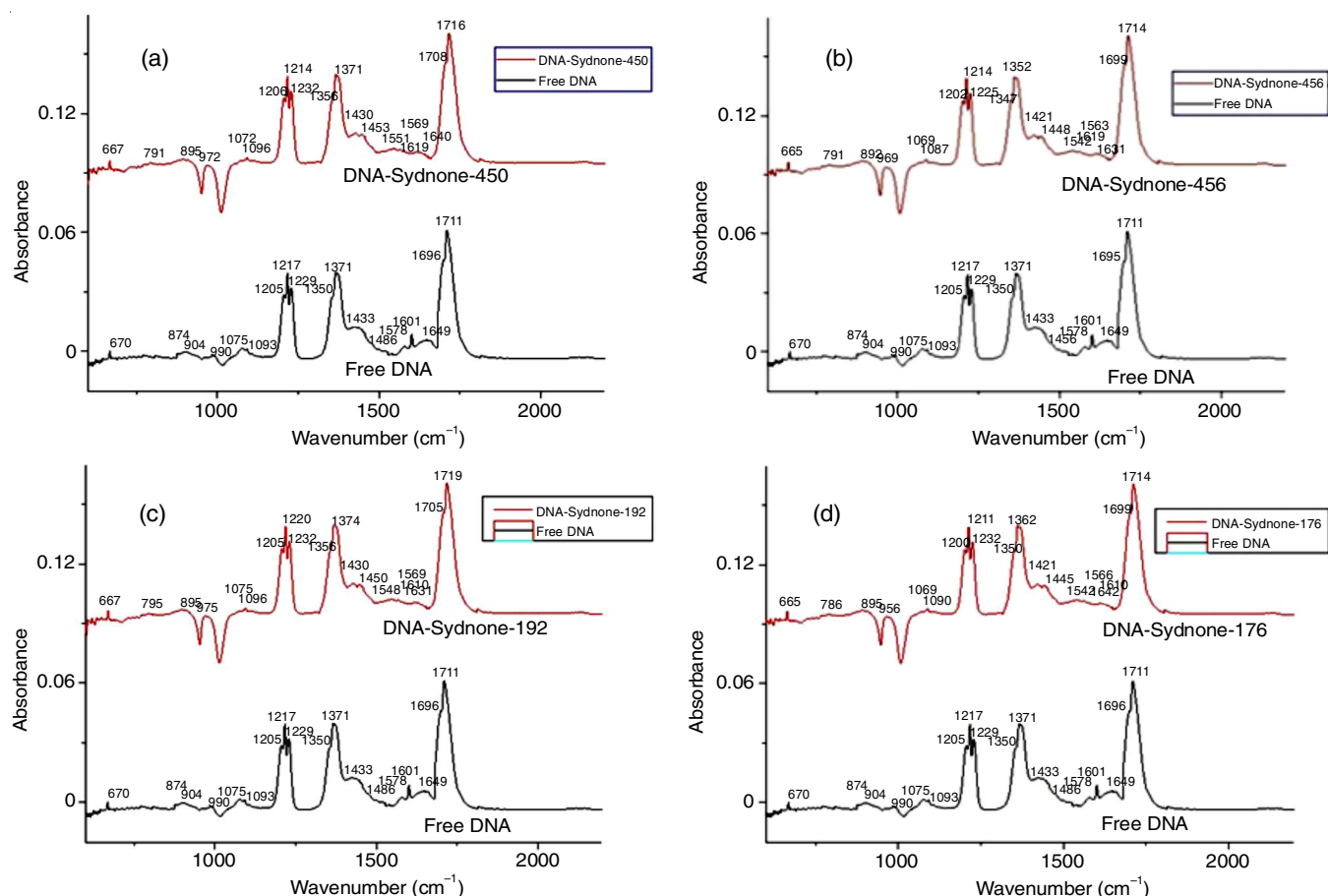

Fig. 2. Spectra of sydnone-DNA binding studies by FTIR spectroscopy [a, b, c and d represent the FTIR spectra of free DNA and sydnone-DNA complex (A: MC 176, B:MC 192, C:MC450, D:MC 456)]

Base binding: The FTIR spectra indicate the change intensity and shifts of bases guanine (Gua), thymine (Thy), adenine (Ade) and cytosine (Cyt)) after interaction of sydnone with DNA, these changes are related to sydnone interaction with DNA base pairs Gua–Cyt and Ade–Thy. The shifting of the bands for MC-176 from 1711 cm^{-1} (Gua) to 1714 cm^{-1}, 1649 cm^{-1} (Thy) to 1642 cm^{-1}, 1601 cm^{-1} (Ade) to 1619 cm^{-1} and 1486 cm^{-1} (Cyt) to 1448 cm^{-1}.

The changes in shifting of the bands for MC-192 at 1711 cm^{-1} (Gua) to 1719 cm^{-1}, 1649 cm^{-1} (Thy) to 1631 cm^{-1}, 1601 cm^{-1} (Ade) to 1619 cm^{-1} and 1486 cm^{-1} (Cyt) to 1450 cm^{-1}. For MC-450 at 1711 cm^{-1} (Gua) to 1716 cm^{-1}, 1649 cm^{-1} (Thy) to 1640 cm^{-1}, 1601 cm^{-1} (Ade) to 1619 cm^{-1} and 1486 cm^{-1} (Cyt) to 1453 cm^{-1} were observed. For MC-456 the shifting for the bands at 1711 cm^{-1} (Gua) to 1714 cm^{-1}, 1649 cm^{-1} (Thy) to 1631 cm^{-1}, 1601 cm^{-1} (Ade) to 1619 cm^{-1} and 1486 cm^{-1} (Cyt) to 1450 cm^{-1}. Upon DNA-sydnone complexation, the guanine band (1711 cm^{-1}) and adenine band (1601 cm^{-1}) shifted towards a higher frequency in all the compounds. Similarly, the thymine band (1649 cm^{-1}) and cytosine band (1486 cm^{-1}) shifted towards the lower frequency for all the compounds. The shift in bands is due to sydnone intercalated to DNA because of change in vibrational forces, which modifies the bases. The change in the vibrational forces is because sydnone is known for good electron acceptor with high polarization ability and dipole moment values. Although Ade–Thy and Gua–Cyt base pairs are good electron donors, which are favourable for the aromatic stacking interactions between DNA and sydnone [36]. Similar effect was observed in known intercalating agents like thiazolo pyrimidine ethidium bromide, acridine orange and methylene blue compounds could successfully fitting into the minor rooves and bind with AT base pairs [32,37].

Phosphate binding: The spectra of free calf thymus DNA (Fig. 2a) the phosphate symmetric vibrations bands are observed at 1093 cm^{-1} [29-31] and the phosphate asymmetric stretching at 1217 cm^{-1}. After the sydnone-DNA complexation, phosphate band at 1093 cm^{-1} shifts to 1096 cm^{-1} and for MC-450 and MC-192. For MC-450 band at 1217 cm^{-1} shifts to 1214 cm^{-1}, for MC-192 band at 1217 cm^{-1} shifts to 1220 cm^{-1}. For MC-176 band at 1093 cm^{-1} shifts to 1090 cm^{-1} and at 1217 cm^{-1} shifts to 1211 cm^{-1}. For MC-456 band at 1093 cm^{-1} shifts to 1096 cm^{-1} 1217 cm^{-1} shifts to 1214 cm^{-1}. These spectral changes in the phosphate stretching specify that sydnone bind to phosphate group of DNA as shown in Fig. 2. This recognized to the external binding of sydnone compounds to phosphate in DNA helix [29].

MTT assay: MTT test was conducted to find the cyto-toxicity of sydnone compounds (MC-176, MC-192, MC-450, MC-456) on BT 474 and the HeLa cell line. All the compound showed dose dependent activity, IC$_{50}$ (half maximal inhibitory concentration) values are shown Table-2. All the compounds found to possess IC$_{50}$ values lower than 50 μM against the HeLa and BT 474 cell line except compound MC-450, which showed 75 μM on Hela cell line. The sydnone compound MC-176 showed remarkable antitumor activity against HeLa cell line and BT 474 cell line with an IC$_{50}$ value of 1.3 μM and 7.08 μM. MC-192 found to be the cytotoxic on the BT 474 and HeLa cell line with an IC$_{50}$ value of 11.46 μM and 19.74 μM.

TABLE-2 IC$_{50}$ VALUES		
Compound	IC$_{50}$ (μM) in HeLa cell line	IC$_{50}$ (μM) in BT 474 cell line
MC-176	7.08	1.30
MC-192	19.74	11.46
MC-450	75.53	24.90
MC-456	46.41	44.83

In some heterocyclic molecule like benzothiazole, isoxa-zole, quinoline and anthracene moieties linked to the respective thiophene derivatives exhibited IC$_{50}$ lower than 50 μM [11]. Several new thiazoles linked nitrogen mustard heterocycles have just proven to have inhibitory effects on panel of human cancer cell lines (MV4-11, A549, HCT116 and MCF-7). Similar thiozole derivative like methane sulfonamide, shown strong inhibitory effect in human leukaemia HCT116 and MCF7 cells with IC$_{50}$ value of 5.48 μM and 4.53 μm [38].

All sydnone compounds found to possess IC$_{50}$ values lower than 50 μM against the HeLa and BT (Breast tumor) 474 cell lines. The cytotoxic activity of sydnone could be because of the heterocyclic structure of sydnone compounds, which has different regions of positive and negative charges. These charges are connected with a poly-heteroatomic system, this make sydnone molecule to cross cellular membranes and may have strong interaction with DNA or proteins [6]. The similar cyto-toxic effect was reported on 1,3,4-thiadiazolium mesoionic compound on human melanoma [17] and sydnone 1: A meso-ionic compound have antitumor effect on Walker-256 carcino-sarcoma and reduced tumour growth by 54% [39].

Determination of apoptosis and necrosis using fluore-scence microscopy: The cytotoxicity of sydnone could be of apoptosis or necrosis. Assessment of apoptosis is vital to distin-guish it from necrosis. Apoptotic cell death includes cellular morphological changes like membrane blebbing, formation of apoptotic bodies, contracted and emarginated nuclei in contrast to normal cell nucleus, which provide the evidence for apoptotic activity of compounds [15]. DAPI (a fluorescent DNA-binding agent), Annexin V and PI staining techniques were used to determine the qualitative identification of apoptic and nectrotic death against both BT 474 breast cancer and the HeLa cell lines. In identifying apoptosis, Annexin V is a protein which is conjugated to a green florescent dye and PI is a red fluorescent dye that stains DNA of both necrotic and late apop-totic cells with damaged membranes. Fluorescence microscopy was used to identify of both apoptotic and necrotic death qualitative and quantitatively.

Anticancer screening results indicated that all compounds were active in MTT assay. All the sydnone compounds at their IC$_{50}$ concentrations were incubated with HeLa and BT cells and performed apoptosis assay and observed under fluore-scence microscope. If the cells are pink coloured with PI, the cells are necrotic. If the cells are coloured green with annexin V were found to be apoptotic cells. Live cells will not take any colour (Annexin V$^-$/PI$^-$), apoptotic cells and late apoptotic (Annexin V$^+$/PI$^-$) are green and necrotic cells (AnnexinV$^-$/PI$^+$) are pink. The results indicated that all the compounds showed maximum apoptotic and late apoptotic activity with both Hela

and BT 474 cell lines as shown in Figs. 3 and 4, except MC-450 which showed necrotic effect at IC_{50} concentration (75.53 µM) in Hela cell line. The percentage of apoptotic and necrotic cells determined for BT 474 breast cancer and Hela cell lines
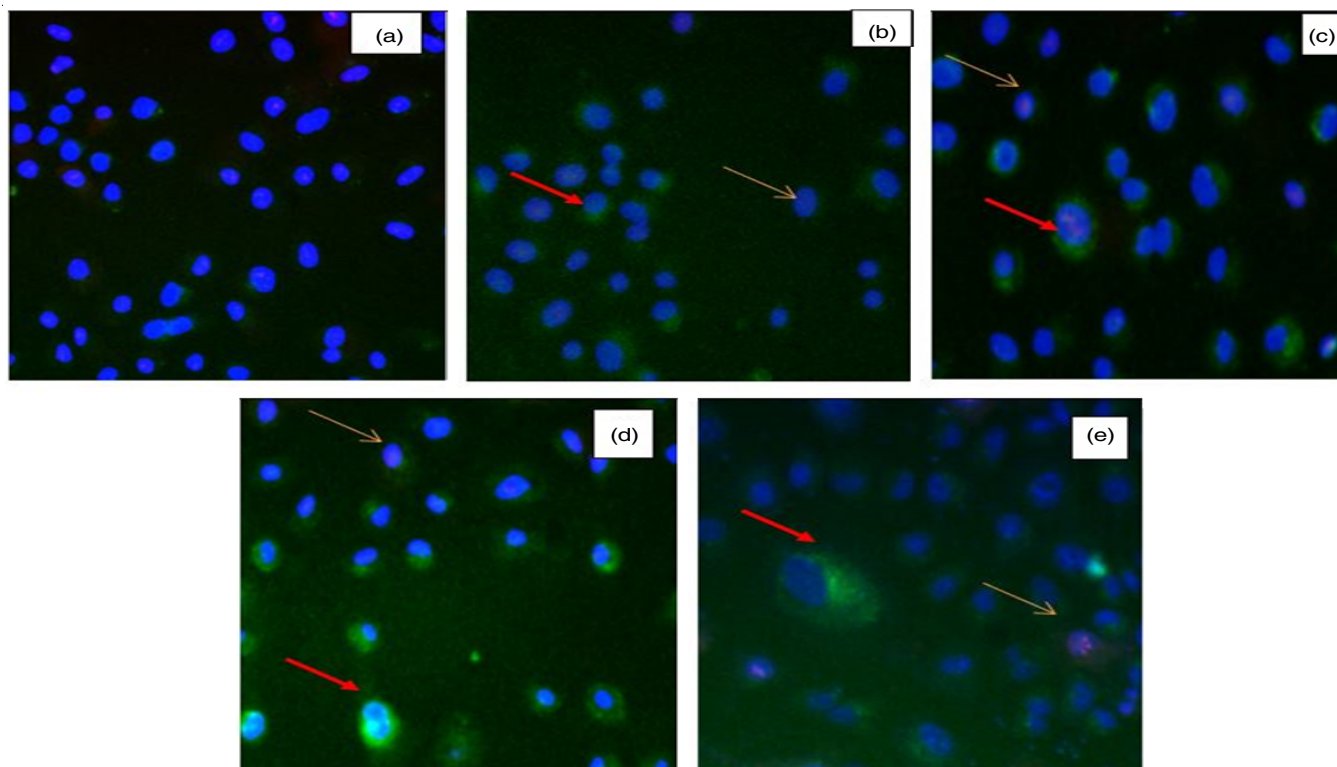
Fig. 3. Apoptosis and necrosis in BT- 474 cells [a: Control-BT 474 breast cancer cell with DAPI staining, b: MC 176, c: MC 192, d: MC 450 and e: MC 456 represent different compounds were treated with BT 474 breast cancer cells in the IC_{50} value (red arrows indicate apoptotic cells and Yellow arrows indicate necrotic cell)]
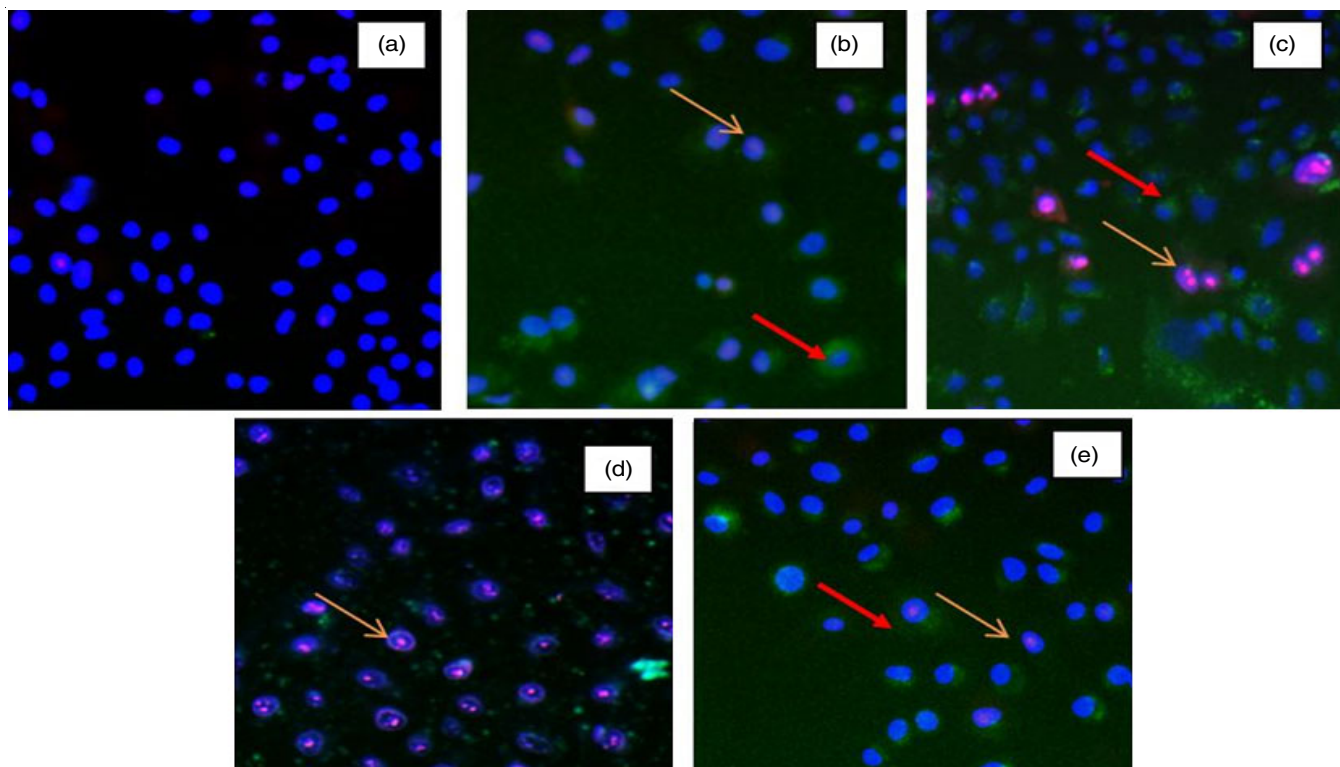

Fig. 4. Apoptosis and necrosis in HeLa cell lines [a: Control-HeLa with DAPI staining, b: MC 176, c: MC 192, d: MC 450 and e: MC 456 (red arrows indicate apoptotic cells and yellow arrows indicate necrotic cell)]

as shown in Table-3. all the sydnone compounds shown apoptosis effect, except MC-450, which was having 43% of necrotic cells compared to other sydnone compounds.

Optimization of sydnone derivatives by Lipinski's rule: "Lipinski's rule of five" is to determine the drug-likeness of a chemical compounds with a specific pharmacological property which would implement it an orally active drug. All the compounds of the present study met the requirements of "Lipinski's rule of five". The other significant property is the total polar surface area (TPSA), TPSA of a compound should be less than140 Å. "Lipinski rule of five" properties of sydnone compounds are listed in Table-4.

Molecular docking analysis: The molecular docking results showed crucial information regarding the orientation of the sydnone compounds in the binding pocket of the target protein. All the sydnone derivatives were docked with tumor associate proteins like Caspase 3 and EGFR-TK, which is highly expressed during uncontrolled cell proliferation. The minimum binding energy indicated that the target proteins, Epidermal Growth Factor Domain Receptor-Tyrosine Kinase (EGFR-TK) and Caspase 3 binds with sydnones compounds. Molecular

docking study showed good interaction of sydnone derivatives with targeted cancer inducing proteins which was compared with the commercially available anticancer drug compound anastrozole. Anastrozole is a non-steroidal inhibitor of estrogen synthesis, which resembles paclitaxel in the chemical structure.

Caspase 3: The predicted active site amino acids in caspase 3 are 29SER, 29SER, 30GLY, 31 ILE, 32 SER, 32SER 33LEU, 33LEU, 33LEU, 33LEU, 33LEU, 33LEU, 34ASP, 35ASN, 35ASN, 36SER, 36SER, 36SER. In the results of molecular docking analysis 3-(4-biphenyl-4′-yl)sydnone (MC-450) compound found to have high molecular energy (-6.48) interaction with Caspase 3 followed by MC-456 > MC-192 > MC-176 sydnone compounds. The detailed molecular confirmations, hydrophobic interactions, hydrogen bond interactions, Salt bridge interactions are shown in Fig. 5, while its values are tabulated in Tables 5-8.

EGFR-TK active site: The predicted active site amino acids in EGFR-TK are 694 LEU, 694 LEU, 694 LEU, 694 LEU, 694 LEU, 695 GLY, 696 SER, 696 SER, 696 SER, 697 GLY, 697 GLY, 698 ALA, 699 PHE, 699 PHE. The molecular docking analysis of 3-(4-butylbiphenyl-4′-yl)sydnone comp-

TABLE-3
THE PERCENTAGES OF APOPTOTIC AND NECROTIC CELLS

	BT 474 breast cancer cell line				Hela cancer cell line				
	Control	MC-176	MC-192	MC-450	MC-456	Control	MC-176	MC-192	MC-450	MC-456
% of Living cell	91.22	47.54	45.30	45.11	46.10	90.00	48.43	49.23	42.20	48.54
% of Apoptotic cell	2.15	48.32	48.54	48.25	44.34	3.15	49.15	45.10	14.36	44.32
% of Necrotic cell	6.63	4.14	6.16	6.64	9.56	5.49	2.42	5.67	43.44	7.44

TABLE-4
LIPINSKI RULE OF 5

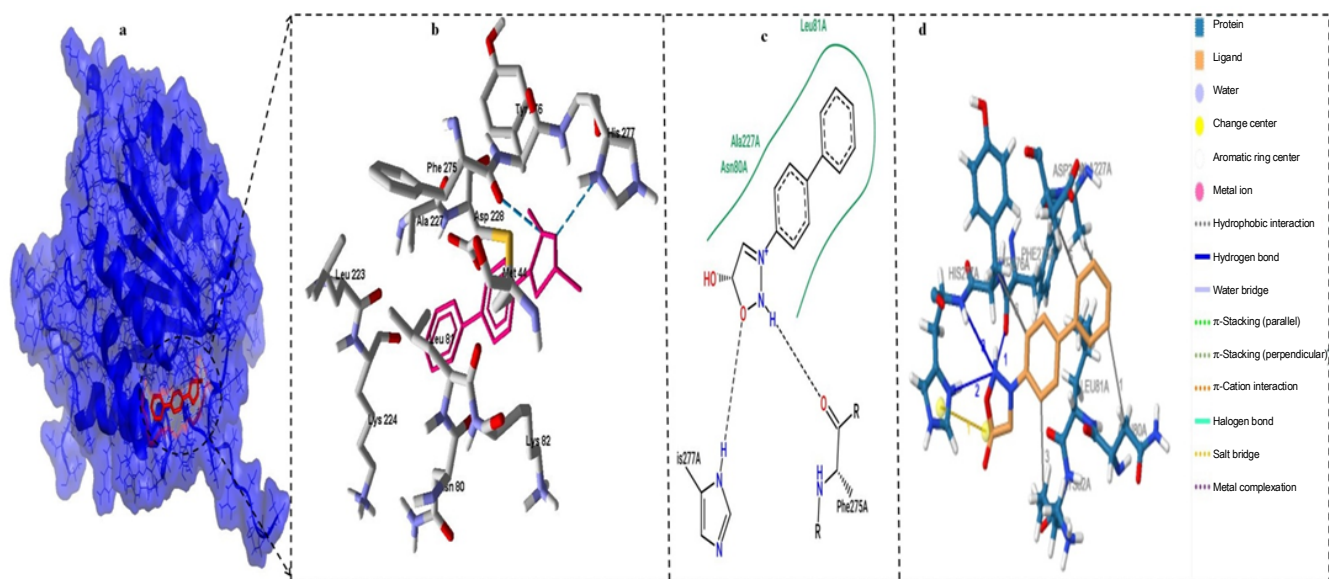| Compound	Chemical Name	HBA	HBD	log P	MW	TPSA
MC-450	3-(4-Biphenyl-4'-yl)sydnone	4	1	-0.04	240.26	47.56
MC-192	3-(4-Octyloxy-2,3-difluorobiphenyl-4'-yl)sydnone	5	1	3.66	404.46	56.79
MC-176	3-(4-Decyloxybiphenyl-4'-yl)sydnone	5	1	4.49	396.53	56.79
MC-456	3-(4-Butylbiphenyl-4'-yl)sydnone	4	1	1.82	296.37	47.56

Fig. 5. 3D and 2D confirmation interactions of 3-(4-biphenyl-4'-yl)sydnone (MC-450) with Caspase 3

TABLE-5
BINDING ENERGY AND HYDROGEN BOND INTERACTION OF SYDNONE
DERIVATIVES AND ANASTROZOLE DOCKED WITH CASPASE 3 AND EGF-TK

Ligands	Chemical name	EGF-TK			Caspase 3		
		Hydrogen bond interaction	No. of H bonds	Energy	Hydrogen bond interaction	No. of H bonds	Energy
MC-450	3-(4-Biphenyl-4'-yl)sydnone	A:GLU738:OE2, A:LYS721:HZ	2	-6.42	A:ARG207:HE, A:ARG64:HH, GLN161:HE	4	-6.48
MC-192	3-(4-Octyloxy-2,3-difluorobiphenyl-4'-yl)sydnone	A:LYS704:HZ	1	-5.46	A:PRO42;O	1	-5
MC-176	3-(4-Decyloxybiphenyl-4'-yl)sydnone	A:MET769:HN	1	-4.53	A:THR237:OG1, A:HIS234:HD	2	-3.49
MC-456	3-(4-Butylbiphenyl-4'-yl)sydnone	A:ASP831:HN	1	-6.44	A:TYR197:HH	1	-6.09
2187	Anastrozole	A:LYS721:HZ	1	-6.41	A:ARG207:HN	1	-6.24

TABLE-6
HYDROPHOBIC INTERACTIONS OF HIGH BINDING ENERGY SYDNONE COMPOUND WITH CASPASE 3 AND EGF-TK

Index	Caspase 3 with 3-(4-biphenyl-4'-yl) sydnone					EGF-TK 3-(4-butylbiphenyl-4'-yl) sydnone				
	Residue	AA	Distance	Ligand atom	Protein atom	Residue	AA	Distance	Ligand atom	Protein atom
1	77A	THR	3.59	3855	731	694A	LEU	3.28	5042	382
2	80A	ASN	3.62	3859	787	702A	VAL	3.89	5050	476
3	81A	LEU	3.37	3857	804	719A	ALA	3.45	5050	763
4	224A	LYS	3.71	3855	2930	768A	LEU	3.22	5042	1531
5	224A	LYS	3.2	3856	2931	820A	LEU	3.35	5051	2393
6	227A	ALA	3.12	3853	2990	820A	LEU	3.51	5053	2392
7	228A	ASP	3.45	3852	3000					

TABLE-7
HYDROGEN BOND INTERACTIONS OF HIGH BINDING ENERGY SYDNONE COMPOUND WITH CASPASE 3 AND EGF-TK

Index	Residue	AA	Distance H-A	Distance D-A	Donor angle	Protein donor?	Sidechain	Donor atom	Acceptor atom
				Caspase 3 with 3-(4-biphenyl-4'-yl) sydnone					
1	77A	THR	1.87	2.66	127.93	×	✓	3850 [Nox]	730 [O3]
2	77A	THR	2.96	3.42	108.19	✓	✓	730 [O3]	3851 [O3]
				EGF-TK 3-(4-butylbiphenyl-4'-yl)sydnone					
1	721A	LYS	3.01	3.53	112.21	✓	✓	796 [N3+]	5044 [Nox]
2	738A	GLU	2.15	2.81	126.69	✓	✓	1073 [O3]	5045 [O3]
3	831A	ASP	2.18	3.1	147.19	✓	×	2577 [Nam]	5039 [O3]

TABLE-8
SALT BRIDGE INTERACTIONS OF HIGH BINDING ENERGY SYDNONE COMPOUND WITH CASPASE 3 AND EGF-TK

Index	Caspase 3 with 3-(4-biphenyl-4'-yl) sydnone						EGF-TK 3-(4-butylbiphenyl-4'-yl)sydnone					
	Residue	AA	Distance	Protein positive?	Ligand group	Ligand atoms	Residue	AA	Distance	Protein positive?	Ligand group	Ligand atoms
1	224A	LYS	5.1	✓	Carboxylate	3848, 3851	721A	LYS	4.9	✓	Carboxylate	5039, 5045

ound (MC-456) with EGFR-TK showed high binding energy (-6.44) followed by other compounds MC-450 > MC-192 > MC-176. The detailed results of molecular confirmations, hydrophobic interactions, hydrogen bond interactions, salt bridge interactions are shown in Fig. 6, while its values are tabulated in Tables 5-8.

ADMET analysis: The potential ADME toxicity profiles of the sydnone compounds were carried out by pkCSM online server with targeted proteins (EGF-TK and Caspase 3) to know whether the sydnone compound have potential pharmacokine-

tics in the human body. All sydnone compounds of ADMET values were compared with commercial anti-breast cancer anastrozole drug molecule. The detailed of each parameter are shown in Table-9.

Conclusion

In this study, the interaction of four sydnone derivatives with calf thymus DNA using UV-visible and FTIR spectroscopic techniques were investigated. The UV-visible spectral changes were observed after the binding of sydnone with DNA.
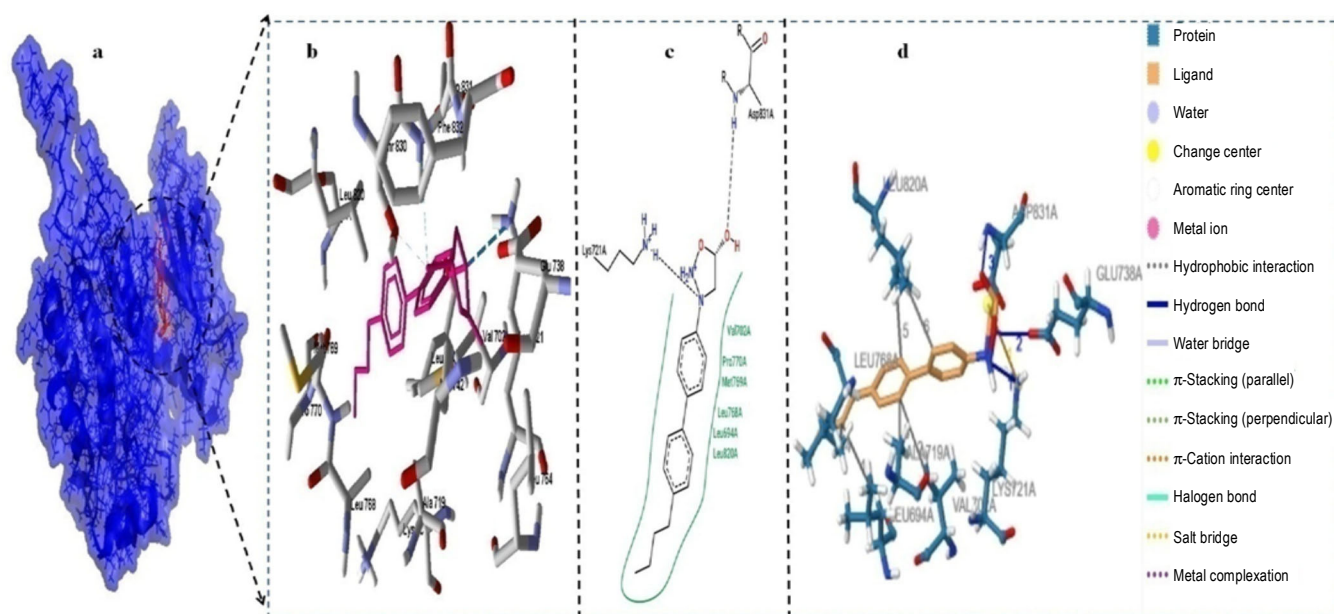
Fig. 6. 3D and 2D confirmation interactions of 3-(4-butylbiphenyl-4'-yl) sydnone (MC-456) with EGF-TK

TABLE-9
ADMET PROFILE OF HIGH ENERGY DOCKED SYDNONE COMPOUNDS

Model name	MC-450 predicted value	MC-192 predicted value	MC-176 predicted value	MC-456 predicted value	Anastrozole predicted value	Unit/Category
Absorption						
Water solubility	-2.65	-6.787	-6.554	-4.215	-3.883	(log mol/L)
Caco2 permeability	1.252	1.243	1.211	1.319	1.022	(log Papp in 10-6 cm/s)
Intestinal absorption (human)	96.854	93.593	92.824	95.955	98.775	(% Absorbed)
Skin Permeability	-2.7	-2.719	-2.677	-2.583	-2.691	(log Kp)
P-glycoprotein substrate	No	Yes	Yes	Yes	No	(Yes/No)
P-glycoprotein I inhibitor	No	Yes	Yes	No	No	(Yes/No)
P-glycoprotein II inhibitor	No	Yes	Yes	No	No	(Yes/No)
Distribution						
VDss (human)	0.246	0.407	0.741	0.621	-0.097	(log L/kg)
Fraction unbound (human)	0.11	0	0	0.028	0.163	(Fu)
BBB permeability	0.095	-0.081	-0.288	-0.023	-0.347	(log BB)
CNS permeability	-1.105	-2.537	-2.527	-1.704	-2.736	(log PS)
Metabolism						
CYP2D6 substrate	No	No	No	No	No	(Yes/No)
CYP3A4 substrate	Yes	Yes	Yes	Yes	Yes	(Yes/No)
CYP1A2 inhibitior	Yes	No	No	Yes	Yes	(Yes/No)
CYP2C19 inhibitior	No	Yes	Yes	Yes	Yes	(Yes/No)
CYP2C9 inhibitior	No	Yes	Yes	No	No	(Yes/No)
CYP2D6 inhibitior	No	No	No	No	No	(Yes/No)
CYP3A4 inhibitior	No	Yes	Yes	No	No	(Yes/No)
Excretion						
Total clearance	0.212	1.253	1.535	0.225	1.525	(log mL/min/kg)
Renal OCT2 substrate	No	No	No	No	No	(Yes/No)
Toxicity						
AMES toxicity	Yes	No	No	No	Yes	(Yes/No)
Max. tolerated dose (human)	-0.075	0.54	0.302	0.255	0.003	(log mg/kg/day)
hERG I inhibitor	No	No	No	No	No	(Yes/No)
hERG II inhibitor	No	Yes	Yes	Yes	No	(Yes/No)
Oral rat acute toxicity (LD50)	2.447	2.439	2.226	2.08	2.363	(mol/kg)
Oral rat chronic toxicity (LOAEL)	1.732	1.992	1.586	0.441	1.338	(log mg/kg_bw/day)
Hepatotoxicity	No	Yes	Yes	No	Yes	(Yes/No)
Skin Sensitization	No	No	No	No	No	(Yes/No)
T. yriformis toxicity	1.186	0.752	0.499	1.231	1.69	(log ug/L)
Minnow toxicity	1	-1.038	-1.342	0.292	1.205	(log mM)

Results affirmed that sydnone partially intercalates between the base pair of DNAs with different binding constants. FTIR results indicate sydnone binding to base guanine and thymine sites. Sydnone also binds externally with the phosphate-sugar backbone of DNA double helix. Sydnone derivatives inhibits cell proliferation and its action is able to induce apoptosis cell death in BT 474 breast cancer and the HeLa human cervical carcinoma cell lines. The molecular docking studies revealed that all the compounds showed good interaction but compound MC-450 and MC-456 showed better docking score within the binding pocket of receptors that was comparable with the standard drug (anastrozole). Drug like properties were justified by Lipinski rule's of five and ADME toxicity properties. Therefore, these sydnone derivatives require to be performed on the animal models to confirm its anticancerous activity.

CONFLICT OF INTEREST

The authors declare that there is no conflict of interests regarding the publication of this article.

REFERENCES

1. H. Sung, J. Ferlay, R.L. Siegel, M. Laversanne, I. Soerjomataram, A. Jemal and F. Bray, *CA Cancer J. Clin.*, **71**, 209 (2021);
https://doi.org/10.3322/caac.21660

2. J.R. Benson, I. Jatoi, M. Keisch, F.J. Esteva, A. Makris and V.C. Jordan, *Lancet*, **373**, 1463 (2009);
https://doi.org/10.1016/S0140-6736(09)60316-0

3. S. Paul, B. Dash, A.J. Bora and B. Gupta, *Int. J. Curr. Pharm. Res.*, **10**, 59 (2018);
https://doi.org/10.22159/ijcpr.2018v10i4.28466

4. C.-C. Tsai, J. Jamison and T. Miller, New Drug Paradigm: Liquid Crystal Pharmaceuticals, Kent State University (2007)
https://www.sciencedaily.com/releases/2007/09/070906135516.htm

5. F. Reinitzer, *Liq. Cryst.*, **9**, 421 (1888);
https://doi.org/10.1007/BF01516710

6. L.B. Kier and E.B. Roche, *J. Pharm. Sci.*, **56**, 149 (1967);
https://doi.org/10.1002/jps.2600560202

7. U. Fischer and K. Schulze-Osthoff, *Pharmacol. Rev.*, **57**, 187 (2005);
https://doi.org/10.1124/pr.57.2.6

8. B. Weber, A. Serafin, J. Michie, C. Van Rensburg, J.C. Swarts and L. Bohm, *Anticancer Res.*, **24(2B)**, 763 (2004).

9. S.W. Fesik, *Nat. Rev. Cancer*, **5**, 995 (2005);
https://doi.org/10.1038/nrc1776

10. M. García-Valverde and T. Torroba, *Molecules*, **10**, 318 (2005);
https://doi.org/10.3390/10020318

11. N. Grynberg, T. Gomes, T. Shinzato, A. Echevarria and J. Miller, *Anticancer Res.*, **12**, 1025 (1992).

12. L.E. Mihajlovic, A. Savic, J. Poljarevic, I. Vuèkovic, M. Bulatovic, M. Mojic, D. Maksimovic-Ivanic, S. Mijatovic, G.N. Kaluderovic, S. Stosic-Grujièic, Ð. Miljkovic, S. Grguric-Šipka and T.J. Sabo, *J. Inorg. Biochem.*, **109**, 40 (2012);
https://doi.org/10.1016/j.jinorgbio.2012.01.012

13. A. Caliskan, H. Karadeniz, A. Meric and A. Erdem, *Anal. Sci.*, **26**, 117 (2010);
https://doi.org/10.2116/analsci.26.117

14. S.K. Kim and B. Nordén, *FEBS Lett.*, **315**, 61 (1993);
https://doi.org/10.1016/0014-5793(93)81133-K

15. B. Nguyen, D. Hamelberg, C. Bailly, P. Colson, J. Stanek, R. Brun, S. Neidle and W. David Wilson, *Biophys. J.*, **86**, 1028 (2004);
https://doi.org/10.1016/S0006-3495(04)74178-8

16. S.T. Saito, G. Silva, C. Pungartnik and M. Brendel, *J. Photochem. Photobiol. B*, **111**, 59 (2012);
https://doi.org/10.1016/j.jphotobiol.2012.03.012

17. A. Senff-Ribeiro, A. Echevarria, E.F. Silva, C.R. Franco, S.S. Veiga and M.B. Oliveira, *Br. J. Cancer*, **91**, 297 (2004);
https://doi.org/10.1038/sj.bjc.6601946

18. J. Wang and L. Urban, *Drug Discov. World Fall*, **5**, 73 (2004).

19. A.P. Li, *Drug Discov. Today*, **6**, 357 (2001);
https://doi.org/10.1016/s1359-6446(01)01712-3

20. S. Usha, I.M. Johnson and R. Malathi, *J. Biochem. Mol. Biol.*, **38**, 198 (2005);
https://doi.org/10.5483/BMBRep.2005.38.2.198

21. W. Tian, C. Chen, X. Lei, J. Zhao and J. Liang, *Nucleic Acids Res.*, **46**, 363 (2018);
https://doi.org/10.1093/nar/gky473

22. G. Hemamalini, P. Jithesh and P. Nirmala, *Int. J. Pharm. Sci. Res.*, **5**, 2374 (2014);
https://doi.org/10.13040/IJPSR.0975-8232.5(6).2374-81

23. T.W. Backman, Y. Cao and T. Girke, *Nucleic Acids Res.*, **9(Web Server issue)**, W486 (2011);
https://doi.org/10.1093/nar/gkr320

24. G.M. Morris, R. Huey, W. Lindstrom, M.F. Sanner, R.K. Belew, D.S. Goodsell and A.J. Olson, *J. Comput. Chem.*, **30**, 2785 (2009);
https://doi.org/10.1002/jcc.21256

25. S. Salentin, S. Schreiber, V.J. Haupt, M.F. Adasme and M. Schroeder, *Nucleic Acids Res.*, **43**, 443 (2015);
https://doi.org/10.1093/nar/gkv315

26. R. Fahrrolfes, S. Bietz, F. Flachsenberg, A. Meyder, E. Nittinger, T. Otto, A. Volkamer and M. Rarey, *Nucleic Acids Res.*, **45**, 337 (2017);
https://doi.org/10.1093/nar/gkx333

27. K. Stierand, P.C. Maass and M. Rarey, *Bioinformatics*, **22**, 1710 (2006);
https://doi.org/10.1093/bioinformatics/btl150

28. E. Taillandier and J. Liquier, *Methods Enzymol.*, **211**, 307 (1992);
https://doi.org/10.1016/0076-6879(92)11018-E

29. D.M. Loprete and K.A. Hartman, *Biochemistry*, **32**, 4077 (1993);
https://doi.org/10.1021/bi00066a032

30. A.A. Ouameur and H.A. Tajmir-Riahi, *J. Biol. Chem.*, **279**, 42041 (2004);
https://doi.org/10.1074/jbc.M406053200

31. D.K. Jangir, S. Charak, R. Mehrotra and S. Kundu, *J. Photochem. Photobiol. B*, **105**, 143 (2011);
https://doi.org/10.1016/j.jphotobiol.2011.08.003

32. M. Tsuboi, *Appl. Spectrosc. Rev.*, **3**, 45 (1970);
https://doi.org/10.1080/05704927008081687

33. S. de Almeida, E. Lafayette, L. da Silva, C. Amorim, T. de Oliveira, A. Ruiz, J. de Carvalho, R. de Moura, E. Beltrão, M. de Lima and L. Júnior, *Int. J. Mol. Sci.*, **16**, 13023 (2015);
https://doi.org/10.3390/ijms160613023

34. G.S. Kumar, M.A. Ali, T.S. Choon and K.J.R. Prasad, *J. Chem. Sci.*, **128**, 391 (2016);
https://doi.org/10.1007/s12039-015-1025-5

35. M. Sirajuddin, S. Ali and A. Badshah, *J. Photochem. Photobiol. B*, **124**, 1 (2013);
https://doi.org/10.1016/j.jphotobiol.2013.03.013

36. S. Nafisi, M. Bonsaii, P. Maali, M.A. Khalil Zadeh and F. Manouchehri, *J. Photochem. Photobiol.*, **100**, 84 (2010);
https://doi.org/10.1016/j.jphotobiol.2010.05.005

37. S. Kasibhatla, G.P. Amarante-Mendes, D. Finucane, T. Brunner, E. Bossy-Wetzel and D.R. Green, *CSH Protocols*, **3**, 4493 (2006);
https://doi.org/10.1101/pdb.prot4493

38. M. Ghorab, M.S. Bashandy and M.S. Alsaid, *Acta Pharm.*, **64**, 419 (2014);
https://doi.org/10.2478/acph-2014-0035

39. L.F. Galuppo, F.A. dos Reis Lívero, G.G. Martins, C.C. Cardoso, O.C. Beltrame, L.M.B. Klassen, A.V.S. Canuto, A. Echevarria, J.E.Q. Telles, G. Klassen and A. Acco, *Basic Clin. Pharmacol. Toxicol.*, **119**, 41 (2016);
https://doi.org/10.1111/bcpt.12545